Supporting Information

Relative Stability of the S_2 isomers of the Oxygen Evolving Complex of Photosystem II

Divya Kaur[1,2], Witold Szejgis[2], Junjun Mao[2], Muhamed Amin[3], Krystle M. Reiss[4], Mikhail Askerka[4], Xiuhong Cai[2,5], Umesh Khaniya[2,5], Yingying Zhang[2,5], Gary W. Brudvig[4], Victor S. Batista[4], M. R. Gunner[1,2,5,*]

[1]*Ph.D. Program in Chemistry, The Graduate Center of the City University of New York, New York, NY 10016, USA*
[2]*Department of Physics, City College of New York, New York 10031, USA*
[3]*University of Groningen, Nijenborgh 4, 9747 AG Groningen, The Netherlands*
[4]*Department of Chemistry, Yale University, New Haven, Connecticut 06520, United States*
[5]*Ph.D. Program in Physics, The Graduate Center of the City University of New York, New York, NY 10016, USA*

I. MCCE results with different input structures.

II. Comparison of calculations in full PSII protein and QM/MM sphere at pH 6.

III. Midpoint potential for oxidation of S_1 to $S_{2,g=2}$ or $S_{2g=4.1}$.

IV. E_m for S_2/S_1 for OEC in full PSII (mV).

V. Determination of position of chloride ion for D2-K317A mutation.

VI. Protonation states of 15Å sphere of residues from the D1, D2, and CP43 subunits with different perturbations.

VII. QM/MM methodology for free energy calculation.

I. MCCE results with different input structures

The protonation states for the OEC and for residues near the cluster were calculated three times in the S_1 and $S_{2,g=2}$ redox states with the same S^1 and $S^{2,g=2}$ structures (n=3) and in the S^1, $S^{2,g=2}$ and $S^{2,g=4.1}$ structures. The average and standard deviation of the protonation states are given Table S1. It also shows the variability when the protonation state is calculated in the same S-state in all three input structures (S^1, $S^{2,g=2}$ and $S^{2,g=4.1}$). In contrast, in Table 2 in the main text the protonation state for a given S-state is calculated in that structure (i.e.S_i^i). In general, the standard deviation is quite small (<0.1 proton). However, D1-E329 is more variable, showing a sensitivity to small changes that makes it able to respond by binding or releasing protons when the OEC is oxidized.

Table S1. Comparison of protonation state changes (change in H^+) for whole PSII in two conditions

	average protonation 3443 state in S^1 structure n=3	average protonation 3443 state in S^1, $S^{2,g=2}$ and $S^{2,g=4.1}$ structures	average protonation 3444 state in $S^{2,g=2}$ structure n=3	average protonation 3444 state in S^1, $S^{2,g=2}$ and $S^{2,g=4.1}$ structures
W2 constraint	free	free	free	free
W1	0±0.0	0±0.0	-0.08±0.03	-0.03±0.02
W2	0±0.0	-0.06±0.10	-0.80±0.03	-0.94±0.10
D1-D61	-1±0.0	-0.92±0.09	-0.92±0.03	-0.97±0.02
D1-H337	1±0.0	1±0.0	1±0.0	1±0.0
D1-E329	-0.37±0.35	-0.71±0.04	-0.42±0.38	-0.48±0.06
D1-E65	-1±0.0	-1±0.0	-1±0.0	-1±0.0
D2-K317	1±0.0	1±0.0	1±0.0	1±0.0
Charge (whole protein)	-33.35±0.16	-33.54±0.03	-34.52±0.30	-34.36±0.08
Charge (residues near OEC)	-16.33±0.35	-16.70±0.04	-17.36±0.38	-17.28±0.05
Change in H^+ (From S_1)			-1.03	-0.58

Residues near the OEC whose protonation states change in different S-states. The pH = 6; W2 free to lose a proton and Y_Z is in the ground state.

II. Comparison of calculations in full PSII protein and QM/MM sphere at pH 6

Classical methods such as MCCE can analyze the full PSII, while higher order methods such as QM/MM are limited in the number of atoms that can be included. The protonation states found in the full PSII were compared with those found for the residues in a 15Å sphere centered at the OEC. In the MCCE calculations the fragment of protein is surrounded by solvent with a dielectric constant of $\varepsilon = 80$.

There is more proton loss from the sphere than from the protein for calculations where W2 is free to titrate. When W2 is fixed protonated the difference in the Boltzmann averaged number of protons bound S_1 or either S_2 states is only 0.05 proton. D1-E329 is buried within PSII but it is at the edge of the sphere where it is fully ionized in all redox states. In the isolated sphere, there is only 2-4% proton transfer between W1 and D1-D61. W2 is 0.84%±0.06 hydroxyl in the $S_{2,g=2}$ redox state. The $E_{m,LRA}$ separation between $S_{2,g=2}$ and $S_{2,g=4.1}$ is ≈50 mV smaller than in the full protein. Thus, the fragment of the protein provides results that are similar to that found in the whole protein but have some significant differences.

Table S2. Protonation states of 15Å sphere of residues from the D1, D2, and CP43 subunits in the absence of the rest of full PSII at pH 6, Y_z in the ground state

	S_1^1	$S_{2,g=2}^{2,g=2}$	$S_{2,g=2}^{2,g=2}$	$S_{2,g=4.1}^{2,g=4.1}$
W2 constraint	free	free	H_2O	free
W1	0±0.0	-0.02±0.03	-0.04±0.02	0±0.0
W2	0±0.0	-0.84±0.06	0±0.0	0±0.0
D1-D61	-1±0.0	-0.98±0.03	-0.96±0.02	-0.99±0.01
D1-H337	1±0.0	1±0.0	1±0.0	1±0.0
D1-E329	-0.99±0.0	-0.95±0.006	-0.99±0.0	-1±0.0
D1-E65	-0.96±0.01	-0.96±0.03	-0.99±0.06	-1±0.0
D2-K317	1±0.0	1±0.0	1±0.0	1±0.0
Total charge	-16.94±0.01	-17.74±0.04	-16.97±0.01	-16.98±0.01
Change in H^+ (From S_1)		-0.77	-0.04	-0.05

This table can be compared with Table 1 in the main text where this sphere is docked into the whole protein.

III. Midpoint potential for oxidation of S_1 to $S_{2,g=2}$ or $S_{2g=4.1}$

The measured free energy for oxidation of the OEC includes the energy required to change the geometry of the OEC and protein as well to remove protons in addition to the electron loss (diagonal Fig S1). In MCCE the OEC is held rigid in a geometry optimized in a specified oxidation state. The Linear Response Approximation (Makri 1999) is applied to estimate the effective E_ms. The LRA E_m ($E_{m,LRA}$) is the average of the E_ms derived in the (fixed) oxidized structure ($E_{m,ox}$) and in the reduced structure ($E_{m,red}$), which are the horizontal lines in Fig. S1.

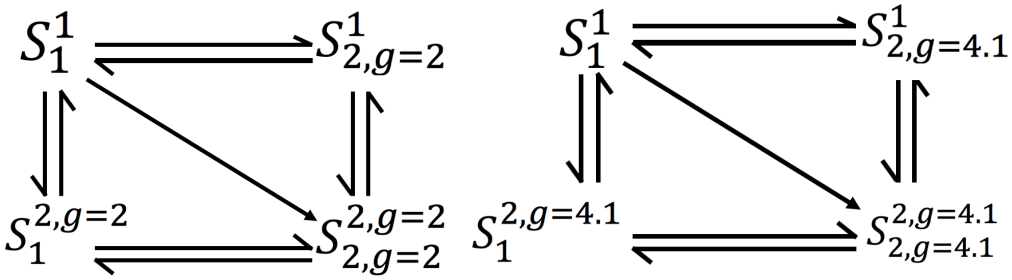

Fig. S1 Thermodynamic square for oxidation of the OEC. The diagonal represents the true reaction where the OEC is free to change structure when it is oxidized. The horizontal reactions are those where oxidation takes place in a fixed structure. S_1^1 is the reduced structure while $S_{2,g=2}^{2,g=2}$ and $S_{2,g=4.1}^{2,g=4.1}$ are the oxidized structures.

IV. E_m for S_2/S_1 for OEC in full PSII (mV)

Table S3

		$S_1^1 \longrightarrow S_{2,g=2}^1$	$S_1^1 \longrightarrow S_{2,g=4.1}^1$	$S_1^{2,g=2} \longrightarrow S_{2,g=2}^{2,g=2}$	$S_1^{2,g=4.1} \longrightarrow S_{2,g=4.1}^{2,g=4.1}$	$S_1^1 \longrightarrow S_{2,g=2}^{2,g=2}$	$S_1^1 \longrightarrow S_{2,g=4.1}^{2,g=4.1}$	$S_{2,g=2}^{2,g=2} \longrightarrow S_{2,g=4.1}^{2,g=4.1}$
	pH	$E_{m,red}$	$E_{m,red}$	$E_{m,ox}$	$E_{m,ox}$	$E_{m,LRA}$	$E_{m,LRA}$	$\Delta E_{m,LRA}$ S_2 isomers
W2 constraint		free/ H_2O	free	free/ H_2O	free	$LRA_{W2:Free}$/ $LRA_{W2:H2O}$	LRA	$LRA_{W2:Free}$/ $LRA_{W2:H2O}$
Ground state	6	1185/ 1555	1845	655/ 685	710	920/ 1120	1278	358/ 158
Cl removed	6	1180/ 1535	1715	495/ 945	645	838/ 1240	1180	343/ -60
$H190^+Y_Z\bullet$	6	1445/ 1670	1970	615/ 845	830	1030/ 1258	1400	370/ 143
Ground state	8	1085/ 1520	1730	535/ 620	585	810/ 1070	1158	348/ 88
D1-D61A	6	1155/ 1210	1855	645/ 740	655	900/ 975	1255	355/ 280
D2-K317A	6	1165/ 1420	1835	645/ 745	685	905/ 1083	1260	355/ 178
D1-S169A	6	1245/ 1535	1835	595/ 670	705	920/ 1103	1270	350/ 168

In each titration involving $S_{2,g=2}$, the top number allows W2 to be free to deprotonate, while the bottom number fixes it as water.

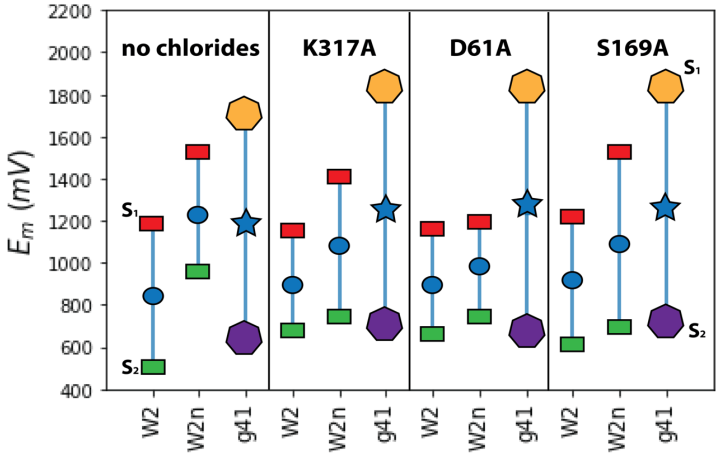

Fig. S2 Relative E_m for oxidation of S_1 to either S_2 state with different modifications of PSII. The $E_{m,LRA}$ for $S_1^1 \longrightarrow S_{2,g=2}^1$ with W2 fixed as water (W2n) is taken as the reference state with an $E_{m,LRA}$ of 1120 mV (Rappaport and Diner 2008). The $E_{m,LRA}$ values given in Table S3. Red rectangle: $S_1^1 \longrightarrow S_{2,g=2}^1$; Yellow heptagon: $S_1^1 \longrightarrow S_{2,g=4.1}^1$;Green rectangle: $S_1^{2,g=2} \longrightarrow S_{2,g=2}^{2,g=2}$. Purple heptagon: $S_1^{2,g=4.1} \longrightarrow S_{2,g=4.1}^{2,g=4.1}$. Blue circle: $E_{m,LRA}$ for S_1 to $S_{2,g=2}$ (average E_m). Blue star: $E_{m,LRA}$ for S_1 to $S_{2,g=4.1}$ (average E_m). Vertical line: range of E_m with S^1 titration at the positive end and either S^2 titration at the lower end. W2: W2 free to ionize in $S_1 \longrightarrow S_{2,g=2}$; W2n: W2 fixed as water S_1 to $S_{2,g=2}$; g41 $S_1 \longrightarrow S_{2,g=4.1}$
Additional perturbations: no chlorides; K317A; D61A; S169A are mutants.

V. Determination of position of chloride ion for D2-K317A mutation

The position of chloride ion (Cl_1) is determined using the translation subroutine in the MCCE (Song and Gunner 2009) program. There are nine additional possible positions for chloride along with the original position near the cavity opened by the D2-K317A mutant. These ions can remain or leave the protein during Grand Canonical Monte Carlo sampling (GCMC). Chloride occupation is calculated using the default concentration of Cl^- =100 mM (Song and Gunner 2009). The results indicate that the occupied position of chloride is 0.5Å away from the original chloride position upon D2-A317 mutation.

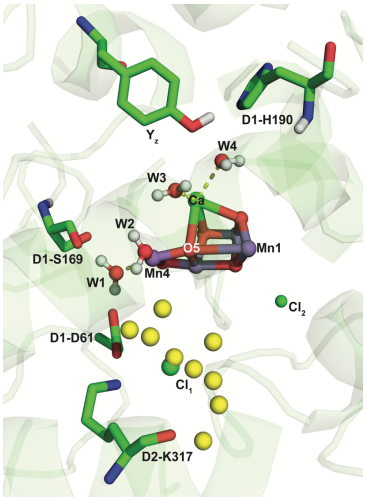

Fig. S3 Sampled positions of Cl_1(color: yellow) with respect to the original position (color: green). Other residues (stick representation): D2-K317, D1-D61, D1-S169 and D1-H190, Y_Z around OEC is under study for calculations. The OEC is in the optimized S_1 (3443) (Luber et al. 2011) configuration as obtained by DFT-QM/MM calculations. The position chosen is the yellow sphere slightly offset from the original, green, Cl.

VI. Protonation states of 15Å sphere of residues from the D1, D2, and CP43 subunits with different perturbations.

Table S4a. pH = 8 and chloride depletion (no CL)

	S_1^1 **pH = 8**	$S_{2,g=2}^{2,g=2}$ **pH = 8**	$S_{2,g=2}^{2,g=2}$ **pH = 8**	$S_{2,g=4.1}^{2,g=4.1}$ **pH = 8**	S_1^1 **no CL**	$S_{2,g=2}^{2,g=2}$ **no CL**	$S_{2,g=2}^{2,g=2}$ **no CL**	$S_{2,g=4.1}^{2,g=4.1}$ **no CL**
W2 constraint	free	free	H_2O	free	free	free	H_2O	free
W1	0	-0.15	-0.26	0	0	-0.28	-0.32	0
W2	0	-0.83	0	0	0	-0.85	0	-0.99
D1-D61	-1	-0.85	-0.74	-1	-0.98	-0.67	-0.68	-0.93
D1-H337	1	1	1	1	0.99	1	1	0.73
D1-E329	-0.98	-0.94	-1	-1	-0.99	-1	-1	-1
D1-E65	-1	-1	-1	-1	-1	-1	-1	-1
D2-K317	1	1	1	1	1	0.79	0	0.93
Charge (whole protein)	-53.39	-54.22	-53.58	-53.61	-34.56	-35.61	-35.61	-35.81
Charge (residues near OEC)	-17.00	-17.77	-17.00	-17.00	-17.00	-18.01	-18.00	-18.26
Change in H^+ (From S_1)		-0.77	0.00	0.00	0.00	-1.01	-1.00	-1.26

Table S4b. D2-K317A and D1-D61A mutation

	S_1^1 **K317A**	$S_{2,g=2}^{2,g=2}$ **K317A**	$S_{2,g=2}^{2,g=2}$ **K317A**	$S_{2,g=4.1}^{2,g=4.1}$ **K317A**	S_1^1 **D61A**	$S_{2,g=2}^{2,g=2}$ **D61A**	$S_{2,g=2}^{2,g=2}$ **D61A**	$S_{2,g=4.1}^{2,g=4.1}$ **D61A**
W2 constraint	free	free	H_2O	free	free	free	H_2O	free
W1	0	-0.09	-0.18	0	0	-0.46	-1	0
W2	0	-0.87	0	-0.68	0	-0.53	0	-1
D1-D61	-0.45	-0.36	-0.76	-0.32	-	-	-	-
D1-H337	1	1	1	1	1	1	1	1
D1-E329	-0.71	-0.85	-0.97	-1	-0.96	-0.95	-1	-1
D1-E65	-0.52	-0.70	-0.19	-0.68	-0.98	-1	-1	-1
D2-K317	-	-	-	-	1	1	1	1
Charge (whole protein)	-33.60	-35.00	-34.25	-34.88	-33.12	-34.11	-34.11	-34.20
Charge (residues near OEC)	-16.70	-17.87	-17.10	-17.68	-16.00	-16.94	-17.00	-17.00
Change in H^+(From S_1)		-1.17	-0.40	-0.98		-0.94	-1.00	-1.00

Table S4c. D1-S169A mutation

	S_1^1	$S_{2,g=2}^{2,g=2}$	$S_{2,g=2}^{2,g=2}$	$S_{2,g=4.1}^{2,g=4.1}$
W2 constraint	free	free	H_2O	free
W1	0	-0.04	-0.08	-0.02
W2	0	-0.77	0	-0.02
D1-D61	-1	-0.96	-0.92	-0.98
D1-H337	1	1	1	1
D1-E329	-0.63	-0.48	-0.98	-1
D1-E65	-1	-1	-1	-1
D2-K317	1	1	1	1
Charge (whole protein)	-33.50	-34.28	-34.13	-34.19
Charge (residues near OEC)	-16.60	-17.25	-16.98	-17.02
Change in H^+(From S_1)		-0.65	-0.38	-0.42

VII. QM/MM methodology for free energy calculation

The QM/MM model consists of the OEC and a 15Å sphere of residues from the D1, D2, and CP43 subunits, as described above and in previous work (Pal et al. 2013; Askerka et al. 2014). The QM layer consists of 10 residues (**D1**-D61, D170, E189, H332, E333, H337, D342, A344 and **CP43**-E354, R357) and 10 water molecules, including the 4 bound substrate waters. Optimizations and frequency calculations were performed using the ONIOM (Vreven and Morokuma 2000) method in the Gaussian 09 (Frisch et al. 2016) software package. The AMBER (Cornell et al. 1995; Case et al. 2012) force field was used for all atoms in the MM layer and DFT/B3LYP (Becke 1988, 1993) for all atoms in the QM layer. The calcium and manganese metal centers were calculated using the LanL2DZ (Hay and Wadt 1985; Wadt and Hay 1985) basis and pseudopotential, and hydrogen, carbon, nitrogen, and oxygen using 6-31G(d) (Ditchfield et al. 1971; Hariharan and Pople 1973). Non-protein heavy atoms in the MM layer (e.g. chloride anions) were frozen in place, as were the capping residues at the edge of the model. All other atoms, including the entire QM layer, were free.

References

Askerka M, Wang J, Brudvig GW, Batista VS (2014) Structural changes in the oxygen-evolving complex of photosystem II induced by the S_1 to S_2 transition: A combined XRD and QM/MM study. Biochemistry 53:6860–6862. doi: 10.1021/bi5011915

Becke AD (1988) Density-functional exchange-energy approximation with correct asymptotic behavior. Phys Rev A 38:3098–3100. doi: 10.1103/PhysRevA.38.3098

Becke AD (1993) Density-functional thermochemistry. III. The role of exact exchange. J Chem Phys 98:5648–5652. doi: 10.1063/1.464913

Case DA, Darden T A, Cheathem TE, et al (2012) AMBER 12, University of California, San Francisco.

Cornell WD, Cieplak P, Bayly CI, et al (1995) A second generation force field for the simulation of proteins, nucleic acids, and organic molecules. J Am Chem Soc 117:5179–5197. doi: 10.1021/ja00124a002

Ditchfield R, Hehre WJ, Pople JA (1971) Self-consistent molecular-orbital methods. IX. An extended gaussian-type basis for molecular-orbital studies of organic molecules. J Chem Phys 54:724–728. doi: 10.1063/1.1674902

Frisch MJ, Trucks GW, Schlegel HB, et al (2016) G09 | Gaussian.com

Hariharan PC, Pople JA (1973) The influence of polarization functions on molecular orbital hydrogenation energies. Theor Chim Acta 28:213–222. doi: 10.1007/BF00533485

Hay PJ, Wadt WR (1985) Ab initio effective core potentials for molecular calculations. Potentials for K to Au including the outermost core orbitals. J Chem Phys 82:299–310. doi: 10.1063/1.448975

Luber S, Rivalta I, Umena Y, et al (2011) S_1-state model of the O_2-evolving complex of photosystem II. Biochemistry 50:6308–6311. doi: 10.1021/bi200681q

Makri N (1999) The linear response approximation and its lowest order corrections: An influence functional approach. J Phys Chem B 103:2823–2829. doi: 10.1021/jp9847540

Pal R, Negre CF, Vogt L, et al (2013) S_0-state model of the oxygen-evolving complex of photosystem II. Biochemistry 52:7703–7706. doi: 10.1021/bi401214v

Rappaport F, Diner BA (2008) Primary photochemistry and energetics leading to the oxidation of the Mn_4Ca cluster and to the evolution of molecular oxygen in photosystem II. Coord Chem Rev 252:259–272. doi: 10.1016/j.ccr.2007.07.016

Song Y, Gunner MR (2009) Using multiconformation continuum electrostatics to compare chloride binding motifs in α-amylase, human serum albumin, and omp32. J Mol Biol 387:840–856. doi: 10.1016/j.jmb.2009.01.038

Umena Y, Kawakami K, Shen J-R, Kamiya N (2011) Crystal structure of oxygen-evolving photosystem II at a resolution of 1.9 Å. Nature 473:55–60. doi: 10.1038/nature09913

Vreven T, Morokuma K (2000) The ONIOM (our own N-layered integrated molecular orbital + molecular mechanics) method for the first singlet excited (S_1) state photoisomerization path of a retinal protonated Schiff base. J Chem Phys 113:2969–2975. doi: 10.1063/1.1287059

Wadt WR, Hay PJ (1985) Ab initio effective core potentials for molecular calculations. Potentials for main group elements Na to Bi. J Chem Phys 82:284–298. doi: 10.1063/1.448800